

# Role of Interface on Dynamic Modulus of High-Performance Poly(etheretherketone)/Ceramic Composites

R. K. Goyal,<sup>1</sup> A. N. Tiwari,<sup>2</sup> Y. S. Negi<sup>3</sup>

<sup>1</sup>Department of Metallurgy and Materials Science, College of Engineering, Pune, 411 005, India

<sup>2</sup>Department of Metallurgical Engineering and Materials Science, Indian Institute of Technology Bombay, Powai, Mumbai 400 076, India

<sup>3</sup>Polymer Science and Technology Laboratory, Department of Paper Technology, Indian Institute of Technology Roorkee, Saharanpur Campus, Saharanpur 247 001, Uttar Pradesh, India

Received 13 March 2010; accepted 16 September 2010

DOI 10.1002/app.33684

Published online 22 February 2011 in Wiley Online Library (wileyonlinelibrary.com).

**ABSTRACT:** High-performance printed circuit board or electronic packaging substrate with low warping particularly at high frequency is the key demand of manufacturers. In the present work, poly(etheretherketone) (PEEK) matrix composites reinforced with untreated micron size aluminum nitride (AlN) and alumina (Al<sub>2</sub>O<sub>3</sub>) particles have been studied for dynamic modulus in the temperature range varying from 30 to 250°C. At 48 vol % particles, the room temperature modulus of the PEEK/AlN composites increased by approximately fivefold (~ 23 GPa), whereas it increased by twofold for PEEK/Al<sub>2</sub>O<sub>3</sub> composite. The reinforcing efficiency is more pronounced at higher temperatures. The significant improvement in modulus was attributed to the better adhesion between the matrix and the AlN particles. Scanning electron microscope (SEM) and Kubat parameter showed that the poor adhesion between the matrix and the

Al<sub>2</sub>O<sub>3</sub> particles resulted in comparatively smaller increase in modulus of PEEK/Al<sub>2</sub>O<sub>3</sub>, despite higher intrinsic modulus of Al<sub>2</sub>O<sub>3</sub> than that of AlN. SEM showed almost uniform distribution of particles in the matrix. The experimental data were correlated with several theoretical models. The Halpin–Tsai model with  $\xi$  (xi) is equal to four correlates well up to 48 vol % AlN composites while  $\xi$  is equal to two correlates only up to 18 vol % Al<sub>2</sub>O<sub>3</sub> composites. Guth–Smallwood model also correlates well up to 28 vol % AlN and 18 vol % Al<sub>2</sub>O<sub>3</sub>-filled composites. Thereafter, data deviated from it due to the particles tendency to aggregate formation. © 2011 Wiley Periodicals, Inc. *J Appl Polym Sci* 121: 436–444, 2011

**Key words:** dynamic mechanical properties; polymer-matrix composites; interface; scanning electron microscope; electronic packaging

## INTRODUCTION

Poly(etheretherketone) (PEEK) matrix composites have widely been used for various applications due to their good chemical resistance, thermal, mechanical, and electrical properties.<sup>1</sup> The addition of ceramic particles into the PEEK matrix has shown significant improvement in thermal and mechanical properties.<sup>2</sup> In electronic process, the thermal load such as cooling, soldering, cycling testing (–65–150°C), or switch on/off of a component is a dynamic process.<sup>3</sup> Hence, dynamic mechanical analyzer has been increasingly used to study dynamic mechanical properties of polymer composites owing to the frequent dynamic-loading situation during use.<sup>4</sup> A high modulus composite is required for low warping and high natural frequency of printed circuit board.<sup>5</sup> The composite modulus is significantly improved by reinforcing fibers or particles in the polymer matrix such as epoxy,<sup>6–8</sup> PEEK,<sup>9–12</sup> poly(tetrafluoroethylene),<sup>13</sup> and poly(vinylidene fluoride)

(PVDF).<sup>14</sup> The modulus increases to an extent proportional to the reinforcing effect, which in turn depends upon loading, size and shape of the reinforcing particles, and nature of the interface. The modulus of polycarbonate/alumina (Al<sub>2</sub>O<sub>3</sub>) or glass beads significantly depends on particle size and increases with decreasing particle size.<sup>15</sup> This is due to the fact that morphology of the polymer matrix adjacent to the particle is different from that of the bulk polymer. This was confirmed by annealing and solid-state nuclear magnetic resonance experiments.<sup>16</sup> Furthermore, the concept was supported by Tsagaropoulos's model, which shows that incorporation of increasing loading of particles into the polymer results in decrease of the average interparticle distance and, thus, constrains polymer chains in the vicinity of the particles.<sup>17</sup> In contrast to this, according to Nakamura et al.,<sup>18</sup> flexural modulus of angular-shaped silica-filled epoxy composites decreases with decreasing mean particle size of silica. Wong et al.<sup>6</sup> reported that the modulus for the epoxy composite increased with increasing particles such as silica-coated aluminum nitride (SCAN), Al<sub>2</sub>O<sub>3</sub>, and SiO<sub>2</sub>. For a given volume fraction of particle, the epoxy/SCAN composite has the highest modulus despite the highest intrinsic

Correspondence to: R. K. Goyal (rkgoyal72@yahoo.co.in).

modulus of  $\text{Al}_2\text{O}_3$ . This was attributed to the greater degree of irregularity in the shape of SCAN when compared with  $\text{Al}_2\text{O}_3$ .

The dynamic mechanical properties of a series of cold crystallized, melt crystallized, and carbon fiber-reinforced PEEK samples have been cited in literature.<sup>19–21</sup> Tregub et al.<sup>22</sup> reported that for a constant carbon fiber-reinforced PEEK composite, the dynamic modulus, strength, and fatigue life are significantly higher than that of sample having lower crystallinity. The presence of crystallinity influences modulus due to the relative constraint imposed on the amorphous phase motions by the crystallites.<sup>23</sup> Recently, we reported the effect of micron-sized aluminum nitride (AlN) particles on the thermal stability, degree of crystallization, and mechanical properties of PEEK matrix.<sup>11,24</sup> Under three-point bending flexural test, the storage modulus of composites determined at bending aspect ratio (i.e., ratio of span length to sample thickness) of 5.5 was found to be much lower than the actual modulus.<sup>11</sup> This is probably due to the shear deformation of the anisotropic or heterogeneous composites at lower bending aspect ratio.<sup>25</sup> To the author's knowledge, there is little published work, which has description on the role of an interface in improving the modulus of high performance particularly PEEK composites.

In view of above, in present study, dynamic mechanical properties of high-performance PEEK matrix composites reinforced with AlN and  $\text{Al}_2\text{O}_3$  ceramic particles using hot pressing were determined at bending aspect ratio of 15. At a constant volume fraction, modulus of both composites was compared and discussed in detail. The experimental data were correlated with several theoretical models. The improvement in modulus was attributed to the quality of interface, which was examined with scanning electron microscopy (SEM) and Kubat parameter. Moreover, modulus of pure PEEK was determined at different aspect ratio varying from 5.5 to 21.

## EXPERIMENTAL

### Materials

The commercial PEEK powder (Grade 5300 PF) obtained from M/s Gharda Chemicals, Gujarat, India, was used as polymer matrix. It has a reported inherent viscosity of 0.87 dL/g measured at a concentration of 0.5 g/dL in concentrated  $\text{H}_2\text{SO}_4$ . The AlN and  $\text{Al}_2\text{O}_3$  powder purchased from Aldrich Chemical Company were used as reinforcements without surface treatment. The particle size range and mean particle size of AlN powder determined with GALAI CIS-1 laser particle size analyzer were 1.5–9.6 and 4.8  $\mu\text{m}$ , respectively. The particle size range and mean particle size of  $\text{Al}_2\text{O}_3$  were 3–15

and 7.8  $\mu\text{m}$ , respectively. As-received absolute ethanol of Merck grade was used for homogenizing the ceramic powder and PEEK powder.

### Procedure for composite preparation

PEEK matrix composites reinforced with 0–70 wt % AlN/ $\text{Al}_2\text{O}_3$  were prepared using the method described in our previous work.<sup>24</sup> Dried powder of AlN or  $\text{Al}_2\text{O}_3$  and PEEK was well premixed through magnetic stirring using an ethanol medium, and the resultant slurry was dried in an oven at 120°C to remove the excess ethanol. Composite samples were prepared from powder by using a laboratory hot press under a pressure of 15 MPa at a temperature of 350°C.

### Characterization

SEM (Philips, XL-30) was used to investigate the morphology of particles, nature of interface, and AlN or  $\text{Al}_2\text{O}_3$  particles distribution in the PEEK matrix. Nature of interface was examined in both polished as well as etched composite sample. A small piece of composite sample was embedded in commercial acrylic-based resin. Sample surfaces were manually ground and polished with successive finer grades of emery papers followed by lapping to remove scratches. For etching, polished samples were etched for 2 min in a 2% w/v solution of potassium permanganate in a mixture of 4 vol of orthophosphoric acid and 1 vol of water. Finally, samples were rinsed well in water and dried. Polished or etched samples were coated with a thin layer of gold using gold sputter coater (Polaron SC 7610, England) and mounted on metal stub, which was grounded with silver paste to minimize charging effects. Dynamic mechanical analyzer (Perkin–Elmer, DMA 7e) was used to carry out the dynamic mechanical properties. The three-point bending fixture consisting of a 15-mm platform and a knife-edge probe was used. The bending aspect ratio, that is, ratio of the span length to sample thickness was about 15. The test was carried out for the temperature range 30–250°C at a heating rate of 5°C/min and frequency of 1 Hz. The samples annealed in a vacuum oven for 2 h at 260°C were mounted in the DMA, and the test was carried out in argon atmosphere under static load of 110 mN and a dynamic load of 100 mN. Before starting the cycle, the samples were held for 5 min at 30°C to stabilize the position of the knife. Moreover, the interfacial adhesion between the particles and polymer matrix was estimated by Kubat parameter (A) using Eq. (1).<sup>26</sup>

$$\text{Kubat parameter}(A) = \{[\tan \delta_c / (V_m \cdot \tan \delta_m)] - 1\} \quad (1)$$

where  $\tan \delta_c$  and  $\tan \delta_m$  are the tangent  $\delta$  (damping) of the composite and matrix, respectively. It is

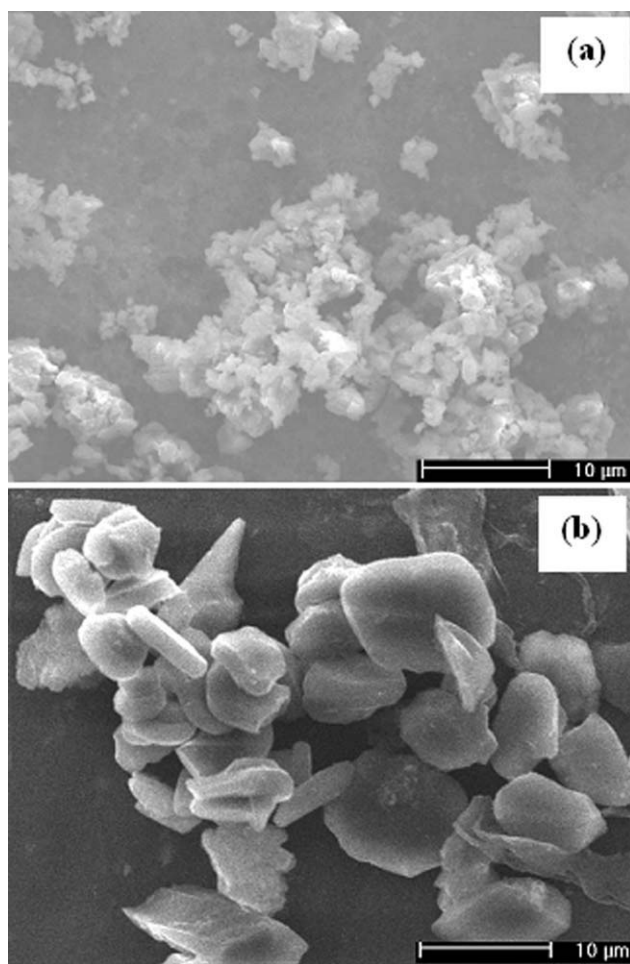


**Figure 1** SEM micrographs of (a) AlN and (b) Al<sub>2</sub>O<sub>3</sub> powder; each scale bar: 10 μm.

reported that  $A$  approaching to 0 corresponds to strong interfacial bonding between the particles and the matrix in the composites.<sup>26</sup>

## RESULTS AND DISCUSSION

### Scanning electron microscopy

The morphological and particle distribution in PEEK matrix were studied using SEM. Figure 1(a,b) shows that the morphology of AlN and Al<sub>2</sub>O<sub>3</sub> is irregular polygonal-shaped and flat platelet-shaped particles, respectively. Figure 2(a–d) shows the SEM of polished PEEK composites reinforced with 30 wt % AlN, 60 wt % AlN, 30 wt % Al<sub>2</sub>O<sub>3</sub>, and 60 wt % Al<sub>2</sub>O<sub>3</sub>, respectively. It can be seen that ceramic particles are almost uniformly dispersed in the PEEK matrix. There are no large aggregates of AlN or Al<sub>2</sub>O<sub>3</sub> in the PEEK matrix, which is expected due to good processing condition. However, particle aggregates consisting of few AlN or Al<sub>2</sub>O<sub>3</sub> primary particles are observed in some regions. This is similar to the results reported by Bikiaris et al.<sup>27</sup> The aggregate formation may be attributed to

the particle–particle interactions due to the decrease in interparticle distance with increasing particle loading. According to Wu, the critical interparticle distance in a polymer/particle system can be determined by

$$\text{C.I.D.} = d[(\pi/6.V_f)^{1/3} - 1] \quad (2)$$

where  $d$  and  $V_f$  are the diameter and volume fraction of particle. Equation (2) shows that interparticle distance depends on the particle diameter and the volume fraction. It decreases with decreasing particle diameter and increasing particle volume fraction.

To study the nature of interfaces between the particles and matrix, SEM images of polished as well as etched samples were taken at higher magnification. Figure 3 shows the SEM of polished surfaces of the PEEK/AlN and PEEK/Al<sub>2</sub>O<sub>3</sub> composites. The interfaces (boundaries) between the AlN particles and the PEEK matrix are indistinct, which are probably the sign of better adhesion between the particles and matrix. In contrast to this, the interfaces between the Al<sub>2</sub>O<sub>3</sub> particles and the matrix are distinct, which may be the sign of poor adhesion. The interfacial interaction between the particles and the matrix was also studied after etching composite samples. Figure 4 shows the SEM of composite samples etched for 2 min. Figure 4(a) shows that the AlN has less angular irregularity than that of pure AlN as shown in Figure 1(a), which may be due to good polymer coating on AlN surface and good interaction between the AlN and the PEEK during processing. Owing to good interaction or adhesion, PEEK was not removed from the AlN particles during etching. Figure 4(b) shows the morphology of etched PEEK/Al<sub>2</sub>O<sub>3</sub> composite. It can be seen clearly that the etching method has leached out the amorphous PEEK and loosely bounded PEEK from the surface and vicinity of Al<sub>2</sub>O<sub>3</sub> particles. Because of poor interaction or adhesion, an etching method results in clearly distinct boundary between the Al<sub>2</sub>O<sub>3</sub> and PEEK matrix. This is in contrast to the PEEK/AlN composite where we did not find any distinct boundary between the AlN and the PEEK. The good adhesion between the AlN and the matrix may be attributed to the irregular polygonal-shaped (hence, higher surface energy) AlN particles, which result in good mechanical interlocking, whereas smooth platelet-shaped Al<sub>2</sub>O<sub>3</sub> particles could not interlock the matrix. In addition, AlN has more affinity to snatch electrons from ketone (C=O) group of PEEK molecule compared to that of Al<sub>2</sub>O<sub>3</sub> particles.

### Dynamic mechanical analysis

Figure 5 shows the storage modulus of pure PEEK as a function of bending aspect ratio (ratio of span length to sample thickness) of the sample. The storage modulus increases with increasing bending



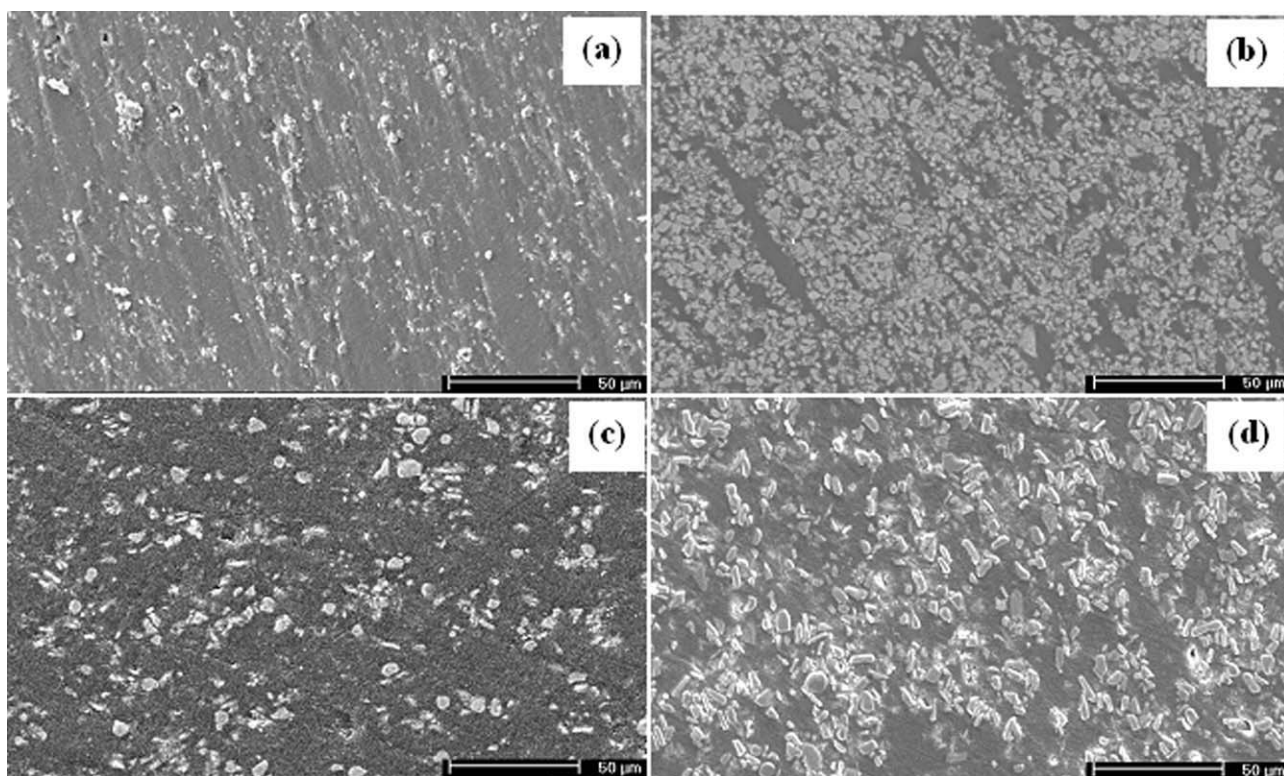


**Figure 2** SEM micrographs of PEEK composites containing (a) 30 wt % AlN, (b) 60 wt % AlN, (c) 30 wt % Al<sub>2</sub>O<sub>3</sub>, and (d) 60 wt % Al<sub>2</sub>O<sub>3</sub>; each scale bar: 50 μm.

aspect ratio. Above aspect ratio of 15, there is a slight increase in storage modulus of PEEK, that is, modulus of pure PEEK determined below bending aspect ratio of 15 is much lower than the true modulus. This is probably due to the shear deformation of the sample.<sup>25</sup> Therefore, all composite samples were characterized at bending aspect ratio about 15 to get the modulus results close to the actual values and hence to minimize the shear deformation during testing. Figure 6 shows storage modulus as a function of temperature for the composites containing AlN from 0 to 70 wt % (48 vol %) AlN. As expected, the storage modulus is increased with AlN content. Moreover, the reinforcing effect is significantly increased at high temperatures, and the storage modulus of all composites exhibits fairly stable values up to 100°C. These results support the previous study of PEEK/CNF composites, where addition of CNF in the PEEK matrix improved modulus both below and above glass transition temperature ( $T_g$ ).<sup>9</sup> However, this is in contrast to short carbon fiber-reinforced PEEK composite, where intense increase in modulus was observed only below  $T_g$  and afterward decreased rapidly similarly to pure PEEK. The authors suggested that this is due to the amorphous nature of the composite as confirmed by X-ray diffraction.<sup>28</sup> A similar trend of storage modulus versus temperature was obtained for PEEK/Al<sub>2</sub>O<sub>3</sub> composites.

Figures 7 and 8 showed room temperature and high temperature (200°C) modulus extracted from modulus versus temperature curves, respectively, for both composites. Figure 7 shows that the modulus of PEEK/AlN composite increases sharply with increasing volume % of AlN whereas that of PEEK/Al<sub>2</sub>O<sub>3</sub> composite gets saturation above 18 vol %. The storage modulus of PEEK reinforced with 48 vol % AlN is increased by about fivefold to 22.8 GPa when compared with 4.7 GPa for pure PEEK at room temperature (30°C) and by about 14-fold to 4.3 GPa when compared with 0.3 GPa for pure PEEK at 200°C (Fig. 8). It is worth noting that the storage modulus of this composite at 30°C is very high, for example, 22.8 GPa, which is comparable to glass fiber-reinforced polymers such as phenolics [Ref. 29, epoxy and polyimide<sup>30,31</sup>] and AlN particles filled PVDF composites.<sup>32</sup> Table I shows the comparison of modulus of PEEK composite with that of other composite's results reported in the literature. The addition of 39 vol % micron size AlN into polystyrene increases the storage modulus by 2.5-fold, that is, from about 2.5 GPa for the pure PS to 6.5 GPa for composite.<sup>33</sup> Ling et al.<sup>34</sup> investigated the cyanate ester/AlN composites and found that the modulus increases by more than twofold at 60 wt % AlN particle content. They also investigated that there is hardly any reinforcing effect of AlN particles above the glass transition of cyanate ester.<sup>34</sup> It is interesting

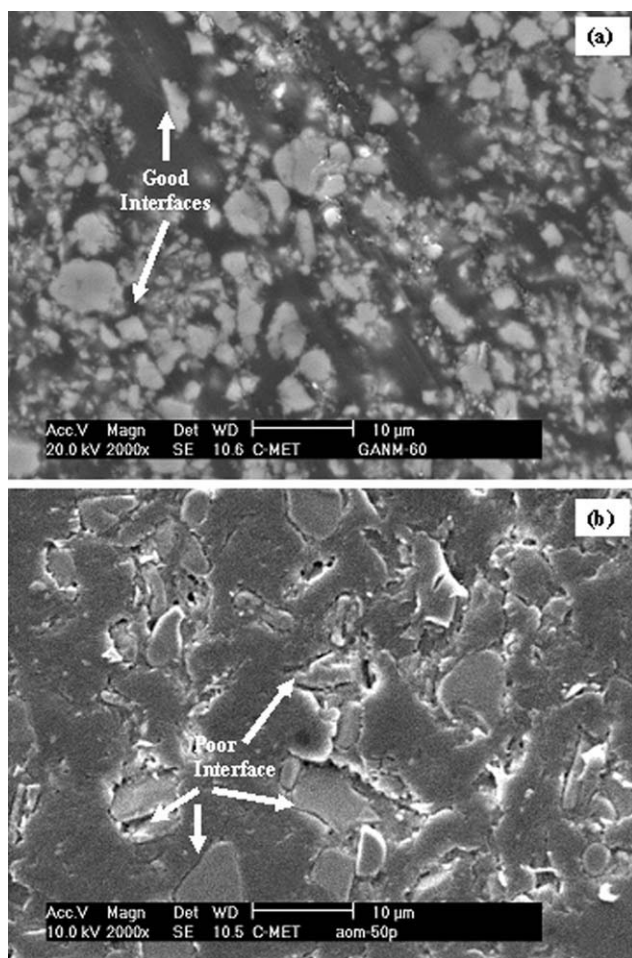


**Figure 3** SEM images of polished samples of (a) PEEK/AlN (60 wt %) and (b) PEEK/Al<sub>2</sub>O<sub>3</sub> (50 wt %) composites, each scale bar: 10 μm.

to see the high modulus of PEEK composites at lower loading than that of literature values. Such a high improvement in modulus of semicrystalline PEEK is most significant.<sup>35,36</sup> Figure 8 shows that the high temperature modulus of both composites increases with increasing volume % of AlN or Al<sub>2</sub>O<sub>3</sub>. It can be seen clearly that AlN is more efficient in improving modulus than that of Al<sub>2</sub>O<sub>3</sub> particles throughout the volume fraction. The ratio of the modulus at 250°C to that at 30°C is 0.07 for pure PEEK, but it increased to 0.19 for 48 vol % PEEK/AlN composites. The modulus is increased due to the high modulus of AlN (308 GPa) and from the good interface formed due to interaction between the AlN particles and the matrix. Furthermore, the Kubat parameter of the composite calculated from the Eq. (1) is given in Table II. It can be seen that Kubat parameter is less than 0, which implies strong interaction between the particles and the matrix. Moreover, irregular-shaped AlN particles may probably be helping in the formation of thick and strong interface as observed in Figure 4(a). The

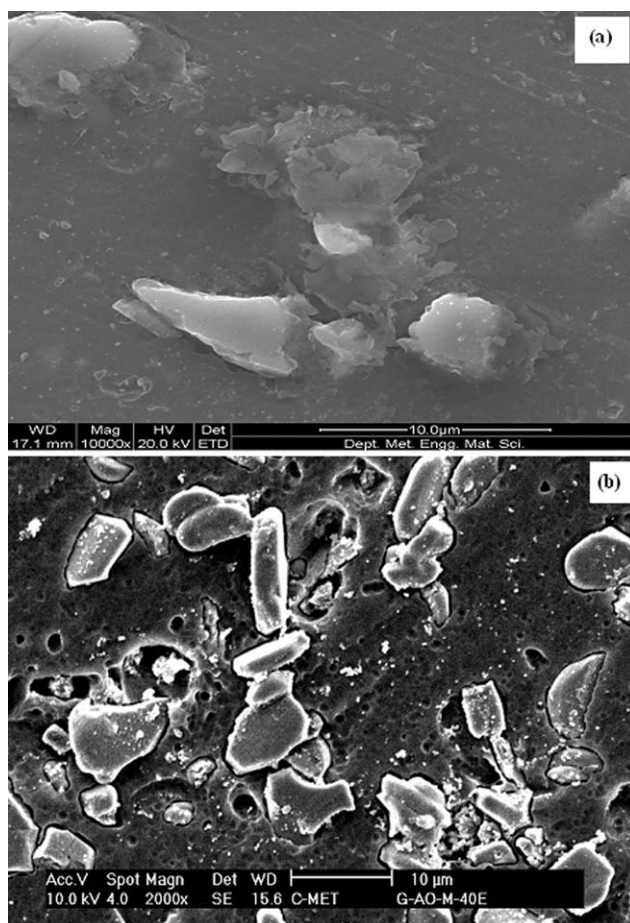


**Figure 4** EM images of etched composite samples of (a) PEEK/AlN and (b) PEEK/Al<sub>2</sub>O<sub>3</sub> composites, scale bar: 10 μm.

resultant strong interface can transfer load from matrix to reinforcing particles.<sup>37,38</sup> Therefore, the significant improvement in storage modulus might be attributed to the good adhesion between the matrix and homogeneously dispersed AlN particles, which restrict segmental motion of the matrix.

The simplest theoretical models to predict the modulus of particle-reinforced polymer composites are the simple rule of mixture (ROM), inverse rule of mixture

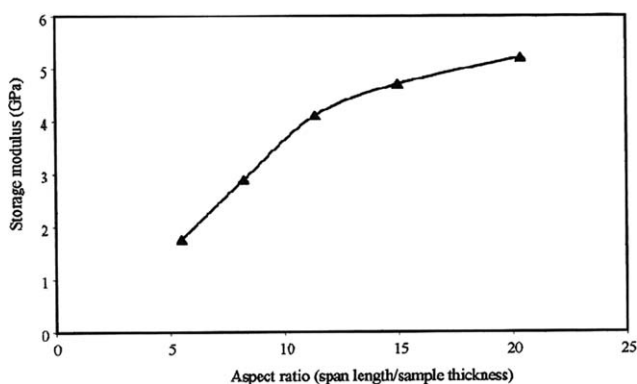


**Figure 5** Effect of bending aspect ratio on storage modulus of pure PEEK.



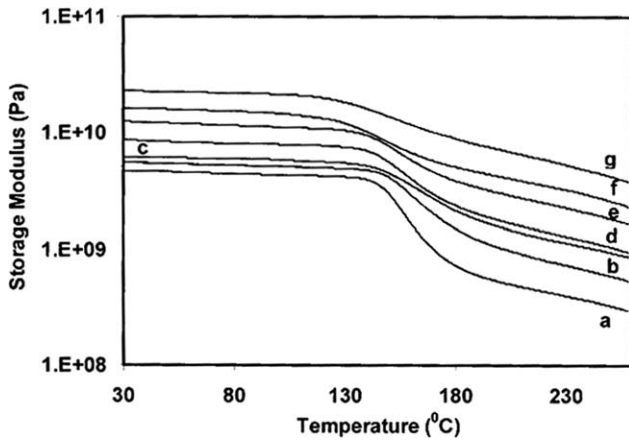


Figure 6 Storage modulus versus temperature for PEEK/AlN composite; (a) pure PEEK, (b) 10 wt %, (c) 20 wt %, (d) 30 wt %, (e) 50 wt %, (f) 60 wt %, and (g) 70 wt % AlN.

(I-ROM), and Einstein's equation.<sup>39</sup> The Einstein equation is valid only at low particle loading when there is perfect adhesion between the particles and the matrix. It is independent of the particle size. It assumes that the particles are very much rigid than that of the matrix. Guth and Smallwood<sup>39</sup> generalized the Einstein concept by introducing a particle interaction term and the modified equation for spherical particle reinforced composites can be represented by Eq. (6). The most versatile equation used for a composite consisting of spherical particles is the Kerner equation.<sup>39</sup> Hashin and Shtrikman model<sup>6</sup> are based on macroscopical isotropy and quasi-homogeneous composites, where the shape of the reinforcing particles is not a limiting factor. This model takes into account the Poisson contraction of the particle and matrix. The lower bound of the model is used for the composites where matrix modulus is lower than particle modulus. Halpin-Tsai model<sup>39,40</sup> is a semiempirical relationship

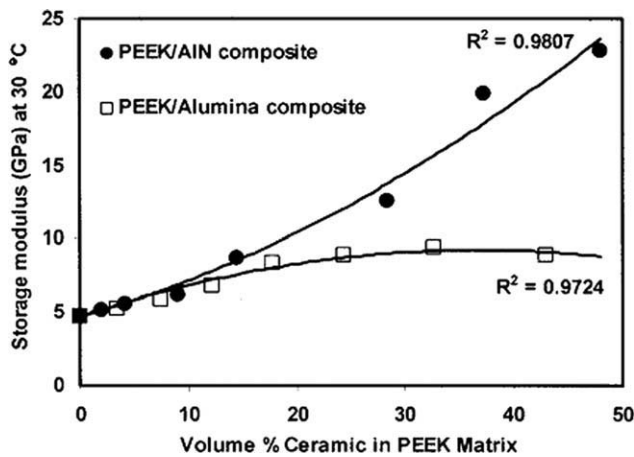


Figure 7 Room temperature storage modulus of composites as a function of volume % of AlN/Al<sub>2</sub>O<sub>3</sub> in PEEK matrix. A good polynomial trend is achieved between the experimental values with a correlation factor  $R^2 > 97\%$ .

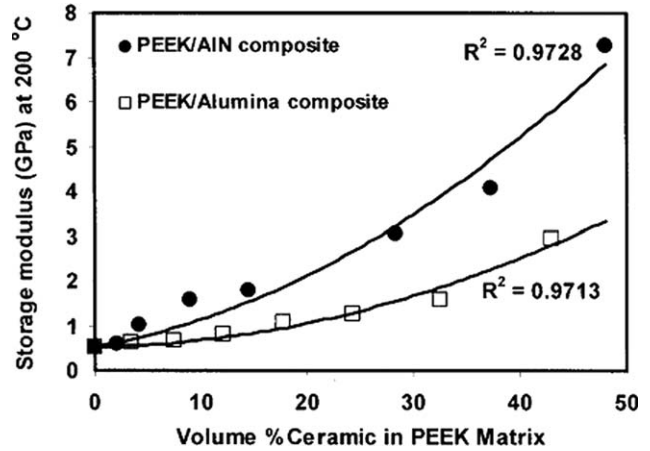


Figure 8 High temperature (200°C) storage modulus of composites as a function of volume % AlN and Al<sub>2</sub>O<sub>3</sub> in PEEK matrix. A good polynomial trend is achieved between the experimental values with a correlation factor  $R^2 > 97\%$ .

that takes into account the aspect ratio of the reinforcing particles. In this, the Poisson ratios of matrix, particles, and encapsulated particles are assumed the same. Lewis and Nielsen<sup>41</sup> modified the Kerner and Halpin-Tsai model by introducing maximum packing fraction ( $\Phi_{max}$ ) term.

$$E_c = E_m V_m + E_f V_f \quad \text{ROM} \quad (3)$$

$$E_c = E_m E_f / (E_m V_f + E_f V_m) \quad \text{I-ROM} \quad (4)$$

$$E_c = E_m [1 + K_E V_f] \quad \text{Einstein} \quad (5)$$

$$E_c = E_m [1 + 2.5 V_f + 14.1 V_f^2] \quad \text{Guth and Smallwood} \quad (6)$$

$$E_c = E_m [1 + 15(1 - \nu_m) / (8 - 10\nu_m) \cdot V_f / (1 - V_f)] \quad \text{Kerner} \quad (7)$$

$$E_c = E_m + \{V_f / [1 / (E_f - E_m) + 3(1 - V_f) / (3E_m + 4G_m)]\} \quad \text{Hashin and Shtrikman} \quad (8)$$

$$E_c / E_m = (1 + \xi \eta V_f) / (1 - \eta V_f) \quad \text{Halpin - Tsai} \quad (9)$$

$$\eta = (E_f / E_m - 1) / (E_f / E_m + \xi)$$

$$E_c / E_m = (1 + ABV_f) / (1 - B\Psi V_f) \quad \text{Lewis and Nielsen} \quad (10)$$

$$B = (E_f / E_m - 1) / (E_f / E_m + 1) \text{ and}$$

$$\Psi = 1 + [(1 - \Phi_{max}) \cdot (1 / \Phi_{max})^2 \cdot V_f]$$

where  $E_c$ ,  $E_f$ , and  $E_m$  are the modulus of the composite, particle, and the matrix, respectively,  $V_f$  and  $V_m$  are the volume fraction of the particle and matrix, respectively, and  $K_E$  is the Einstein coefficient, which is equal to 2.5 for spherical particles. The  $\nu_m$  is the Poisson ratio of the matrix. The  $\xi$  is the adjustable constant, which is equal to 2 for the spherical particles. The upper bound is obtained when  $\xi$  is equal to infinite, and lower bound is obtained when  $\xi$  is

**TABLE I**  
**Comparison of Modulus of PEEK/Ceramic Composites with Literature Values**

| Composites                           | Reinforcements in matrix |                                 | Approx. modulus (GPa) | Reference |
|--------------------------------------|--------------------------|---------------------------------|-----------------------|-----------|
|                                      | vol %                    | Type                            |                       |           |
| Epoxy/Al <sub>2</sub> O <sub>3</sub> | 50                       | particles                       | 12 <sup>a</sup>       | 6         |
| Epoxy/SCAN                           | 50                       | particles                       | 15                    | 6         |
| Epoxy/SiO <sub>2</sub>               | 50                       | particles                       | 10                    | 6         |
| Epoxy/E-glass                        | 60                       | fiber                           | 17.4                  | 30,31     |
| Polyimide/E-glass                    | –                        | fiber                           | 20.9                  | 30,31     |
| PVDF/AlN                             | 60                       | Particles with whiskers         | 15.5                  | 32        |
| Polystyrene/AlN                      | 39                       | Particles                       | 6.5                   | 33        |
| PEEK/AlN                             | 48                       | Irregular shaped particles      | 22.8                  | Exp.      |
|                                      | 37                       |                                 | 19.9                  |           |
| PEEK/Al <sub>2</sub> O <sub>3</sub>  | 43                       | Flat platelets shaped particles | 8.91                  | Exp.      |

<sup>a</sup> Approximate modulus taken from the Figure 12 of ref. 6.

equal to 0. The adjustable constant depends on the geometry and packing of the particles as well as on the direction of the load relative to the orientation of anisotropic particles. For randomly packed spherical particles,  $A$  is equal to 1.5 and  $\Phi_{\max}$  is equal to 0.637.

Figure 9 shows that the storage modulus of PEEK/AlN composites is situated between the upper bound (ROM) and the lower bound (I-ROM). The ROM and I-ROM consider the constituents of the composites under the same strain and stress under the applied load, respectively. However, in particle-reinforced polymer composites, the particles might not be completely separated from one another, and there may be particle aggregates on microlevel as observed in SEM micrographs. Thus, the stress or strain will be distributed unevenly between the particles and aggregates, and the assumption of either uniform strain or stress is an oversimplification.<sup>39</sup> Moreover, these models do not consider size and geometry of the particles and adhesion between the particles and matrix. Hence, experimental modulus lies in between the upper and lower bounds. Einstein model underestimates the modulus values for the composites, because it is valid only at low loading for spherical particle. In reality, AlN particles are irregular/polygonal in shape instead of spherical as shown in Figure 1(a).

Although, Lewis and Neilson model considers the maximum packing fraction of the particles, but it still underestimates the modulus value. The broad particle size distribution (1.5–9.6  $\mu\text{m}$ ) may affect the maximum packing fraction, because particles with

different size can pack more densely than monodispersed particles. Moreover, this model does not take into account the interaction/adhesion between the particle–matrix and particle–particle. The lower bound of the Hashin–Shtrikman (H–S lower) model is useful for the polymer–matrix composite, where modulus of the matrix is lower than that of reinforcing particle but with their lower modulus ratio. In the present case, this also underestimates the modulus of the composites, which may be attributed to the higher modulus ratio ( $\sim 66$ ) of particles to matrix.

Halpin–Tsai model with  $\xi$  is equal to 4 correlates well with the storage modulus of PEEK/AlN composites. This model provides a better estimation for modulus, because (i) it takes into account the aspect ratio and geometry of the particles and (ii) it employs a curve-fitting parameter  $\xi$ , which represents reinforcing efficiency. In other words, the higher value of  $\xi$  (i.e., 4) for the PEEK/AlN composites than that of spherical particles ( $\xi = 2$ ) reinforced polymer matrix also shows that irregular-shaped AlN particles have higher reinforcing efficiency. Guth and Smallwood correlate closely the data up to 28 vol % AlN, which is similar to the results of Cu particles reinforced HDPE composites<sup>42</sup> and surface-treated TiO<sub>2</sub>-reinforced epoxy composites.<sup>43</sup> Hussain et al.<sup>43</sup> investigated that Guth–Smallwood model fits well the modulus of epoxy composites up to 10 vol %-treated TiO<sub>2</sub>. They found that treated TiO<sub>2</sub>-filled composites have modulus higher than that of untreated TiO<sub>2</sub>-filled composites. Thereafter, it overestimates the modulus. This is due to the fact that it assumed perfect

**TABLE II**  
**Kubat Parameter (A) of PEEK/Ceramic Composites**

| Compositions  | Wt % of AlN in composites |      |       |       |       | Wt % of Al <sub>2</sub> O <sub>3</sub> in composites |      |      |      |
|---------------|---------------------------|------|-------|-------|-------|--|------|------|------|
|               | 0                         | 10   | 30    | 50    | 60    | 10   | 30   | 50   | 60   |
| Parameter (A) | 0                         | 0.02 | –0.15 | –0.03 | –0.03 | –0.004   | 0.14 | 0.21 | 0.32 |

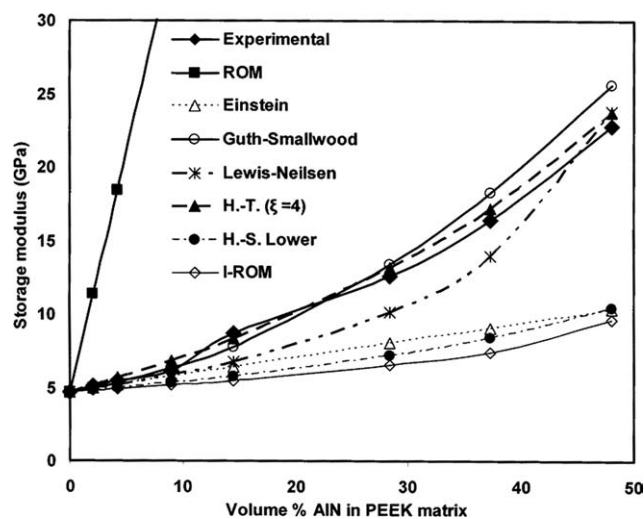


**Figure 9** Comparison of experimental and theoretical modulus of PEEK/AlN composites.

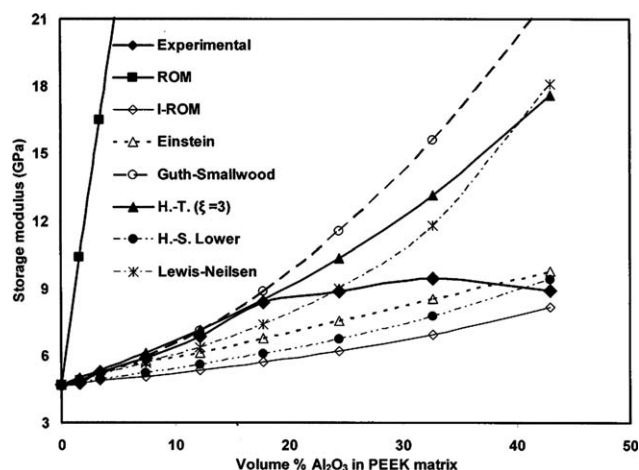
adhesion between the particles and matrix. In reality, perfect adhesion between the particles and matrix is not possible due to the tendency to particle aggregates as the particle loading is increased. Because of the aggregate formation, the effective interfacial area or volume between the AlN particles and matrix, which is responsible for load transfer from matrix to particles, will be less than the actual. Hence, the experimental storage modulus is deviated downward than the predicted modulus.

Figure 10 shows that the storage modulus of PEEK/Al<sub>2</sub>O<sub>3</sub> composites is situated between the ROM and I-ROM. Similar to the PEEK/AlN composites, the ROM, I-ROM, Einstein, Lewis and Neilson, and lower bound of the Hashin-Shtrikman models did not fit the data. However, Halpin-Tsai with  $\xi$  equal to 3 and Guth-Smallwood model correlate well the data up to 18 vol %. Thereafter, the storage modulus is much less than the predicted modulus. The deviation of experimental modulus from these models at higher particle loading might be attributed to the poor adhesion between the Al<sub>2</sub>O<sub>3</sub> particles and PEEK matrix as confirmed from SEM images [Figs. 3(b) and 4(b)], because any model does not consider the effect of porosity and quality of interaction between the particles and matrix. In contrast to PEEK/AlN composites, the modulus of 70 wt % (43 vol %) PEEK/Al<sub>2</sub>O<sub>3</sub> composite is increased only by about twofold at 30°C and by sixfold at 200°C. The comparatively low improvement in modulus of PEEK/Al<sub>2</sub>O<sub>3</sub> composite is despite higher intrinsic modulus of Al<sub>2</sub>O<sub>3</sub> (345 GPa) than AlN (308 GPa). The low improvement in modulus may be attributed to poor adhesion between the Al<sub>2</sub>O<sub>3</sub> and matrix as confirmed from SEM images and increased Kubat parameter. Table II shows that the Kubat parameter calculated for the PEEK/Al<sub>2</sub>O<sub>3</sub> composite is 0.21

and 0.32 for 50 and 60 wt % Al<sub>2</sub>O<sub>3</sub>, respectively, which is much higher than 0. This implies poor adhesion/interaction between the Al<sub>2</sub>O<sub>3</sub> particles and the matrix.

## CONCLUSIONS

We reported on improvement in dynamic mechanical properties of high-performance PEEK matrix composites reinforced with untreated micron-size AlN and Al<sub>2</sub>O<sub>3</sub> ceramic particles ranging from 0 to 70 wt % using hot pressing. The SEM reveals almost uniform distribution of ceramic particles in the matrix. It also reveals that there is good interaction/adhesion between the AlN and the matrix, which resulted in fivefold increase in room temperature modulus of PEEK/AlN composites. This is much comparable than the E-glass fiber/polymer and other particulate composites. However, SEM and Kubat parameter reveal poor adhesion between the Al<sub>2</sub>O<sub>3</sub> and the matrix which resulted in comparatively lower increase in modulus at the same volume fraction. A good interface transfers the load efficiently from the matrix to the particles. It is noteworthy that improvement in efficiency is more pronounced at high temperature, and the composite modulus is fairly stable up to 100°C. The Halpin-Tsai and Guth-Smallwood models can be used to predict the modulus of above system. This study shows that the nature of interface plays the important role than intrinsic properties of constituents in improving properties of composites. We believe that PEEK/AlN composites due to very high modulus and environmentally benign (i.e., it is free from bromine while commercial FR-4 laminate content more than 15% bromine compounds) properties may prove to be the promising materials for high-performance applications particularly in electronic packaging.



**Figure 10** Comparison of experimental and theoretical modulus of PEEK/Al<sub>2</sub>O<sub>3</sub> composites.



We thank Dr. P. D. Trivedi, Polymer Division, Gharda Chemicals, India, for providing PEEK powder for this research work. Dr U.P. Mulik, Sr. Scientist of Centre for Materials for Electronics Technology, Pune, is also acknowledged for his help.

## References

- Frederic, N. C. *Thermoplastic Aromatic Polymer Composites*; Butterworth Heinemann Ltd.: Oxford, 1992.
- Goyal, R. K.; Tiwari, A. N.; Mulik, U. P.; Negi, Y. S. *Compos Sci Technol* 2007, 67, 1802.
- Quella, F.; Bogner, M.; Holzapfel, W.; Schwarz, R. *IEEE Trans Compon Hybrids Manuf Technol* 1991, 14, 8779.
- Yao, X. F.; Yeh, H. Y.; Zhou, D.; Zhang, Y. H. *J Comp Mater* 2006, 40, 371.
- Hegde, S.; Pucha, R. V.; Sitaraman, S. K. *J Mater Sci: Mater Sci* 2004, 15, 287.
- Wong, C. P.; Raja, S. B. *J Appl Polym Sci* 1999, 74, 3396.
- Teh, P. L.; Jaafar, M.; Akil, H. M.; Seetharamu, K. N.; Wagiman, A. N. R.; Beh, K. S. *Polym Adv Technol* 2008, 19, 308.
- Jenness, J. R., Jr.; Kline, D. E. *J Appl Polym Sci* 1973, 17, 3391.
- Sandler, J.; Werner, P.; Sheffer, M. S. P.; Demchuk, V.; Altstädt, V.; Windle, A. H. *Compos A* 2002, 33, 1033.
- Selzer, R.; Friedrich, K. *Compos A* 1997, 28, 595.
- Goyal, R. K.; Tiwari, A. N.; Mulik, U. P.; Negi, Y. S. *Compos A* 2007, 38, 516.
- Goyal, R. K.; Tiwari, A. N.; Mulik, U. P.; Negi, Y. S. *J Appl Polym Sci* 2007, 104, 568.
- Zhang, Z.; Klein, P.; Friedrich, K. *Compos Sci Technol* 2002, 62, 1001.
- Kim, J.-W.; Cho, W.-W.; Ha, C.-S. *J Polym Sci Part B: Polym Phys* 2002, 40, 19.
- Vollenberg, P. H. T.; Heikens, D. *Polymer* 1989, 30, 1656.
- Vollenberg, P. H. T.; Heikens, D. *Polymer* 1989, 30, 1663.
- Tsagaropoulos, G.; Eisenberg, A. *Macromolecules* 1995, 28, 6067.
- Nakamura, Y.; Yamaguchi, M.; Okubo, M.; Matsumoto, T. *J Appl Polym Sci* 1992, 44, 151.
- Melo, J. D. D.; Radford, D. W. *Compos A* 2002, 33, 1505.
- Krishnaswami, R. K.; Kalika, D. S. *Polymer* 1994, 3560, 1157.
- Adam, R. D.; Gaitonde, J. M. *Compos Sci Technol* 1993, 47, 271.
- Tregub, A.; Harel, H. M. *Compos Sci Technol* 1993, 48, 185.
- Jonas, A.; Legras, R. *Macromolecules* 1993, 26, 813.
- Goyal, R. K.; Tiwari, A. N.; Negi, Y. S. *Eur Polym J* 2034 2005, 41.
- Farebrother, T. H.; Raymond, J. A. In *Polymer Engineering Composites*; Richardson, M. O. W., Ed.; Applied Science: London, 1977; pp 197–235.
- Kubat, J.; Rigdahl, M.; Welander, M. *J Appl Polym Sci* 1990, 39, 1527.
- Bikiaris, D. N.; Papageorgiou, G. Z.; Pavlidou, E.; Vouroutzis, N.; Palatzoglou, P.; Karayannidis, G. P. *J Appl Polym Sci* 2006, 100, 2684.
- Hanchi, J.; Eiss, N. S., Jr. *Wear* 1997, 203–204, 380.
- Ishida, H.; Rimdusit, S. *Thermochem Acta* 1998, 320, 177.
- Electronic Materials Handbook, Packaging*, Vol. 1, ASM International Handbook, 1989.
- Tummala, R. R.; Rymaszewski, E. J.; Klopfenstein, A. G., Eds. *Microelectronics Packaging Handbook, Subsystem Packaging, Part 3*, 2nd ed; Chapman & Hall: Netherlands.
- Xu, Y.; Chung, D. D. L.; Mroz, C. *Compos A* 2001, 32, 1749.
- Suzhu, Y.; Peter, H. *J Appl Polym Sci* 2000, 78, 1348.
- Ling, W.; Gu, A.; Liang, G.; Yuan, L.; Liu, J. *Polym Adv Technol* 2009, 21, 365.
- Jin, Z.; Pramoda, K. P.; Xu, G.; Goh, S. H. *Chem Phys Lett* 2001, 337, 43.
- Choi, Y.-K.; Sugimoto, K.-I.; Song, S.-M.; Gotoh, Y.; Ohkoshi, Y.; Endo, M. *Carbon* 2005, 43, 2199.
- Gu, W.; Wu, H. F.; Kampe, S. L.; Lu, G.-Q. *Mater Sci Eng A* 2000, 277, 237.
- Paipetis, S. A. *Fiber Sci Technol* 1980, 13, 449.
- Ahmed, S.; Jones, F. R. *J Mater Sci* 1990, 25, 4933.
- Elias, H.-G. (Ed.). *An Introduction to Plastics*, 2nd ed; Wiley-VCH: Weinheim, 2003.
- Lewis, T. B.; Nielsen, L.E. *J Appl Polym Sci* 1970, 14, 1449.
- Tavaman, I. H. *Powder Technol* 1997, 91, 63.
- Hussain, M.; Nakahira, A.; Nishijima, S.; Niihara, K. *Mater Lett* 1996, 26, 299.